www.czasopisma.pan.pl PAN POLSKA AKADEMIA NAUK www.journals.pan.pl

Arch. Metall. Mater., Vol. 61 (2016), No 1, p. 341–346

DOI: 10.1515/amm-2016-0063

M. RYWOTYCKI*,#, Z. MALINOWSKI*, J. FALKUS*, K. SOŁEK*, A. SZAJDING*, K. MIŁKOWSKA-PISZCZEK*

MODELLING OF HEAT TRANSFER AT THE SOLID TO SOLID INTERFACE

In technological process of steel industry heat transfer is a very important factor. Heat transfer plays an essential role especially in rolling and forging processes. Heat flux between a tool and work piece is a function of temperature, pressure and time. A methodology for the determination of the heat transfer at solid to solid interface has been developed. It involves physical experiment and numerical methods. The first one requires measurements of the temperature variations at specified points in the two samples brought into contact. Samples made of C45 and NC6 steels have been employed in physical experiment. One of the samples was heated to an initial temperature of: 800°C, 1000°C and 1100°C. The second sample has been kept at room temperature. The numerical part makes use of the inverse method for calculating the heat flux and at the interface. The method involves the temperature field simulation in the axially symmetrical samples. The objective function is bulled up as a dimensionless error norm between measured and computed temperatures. The variable metric method is employed in the objective function minimization. The heat transfer coefficient variation in time at the boundary surface is approximated by cubic spline functions.

The influence of pressure and temperature on the heat flux has been analysed. The problem has been solved by applying the inverse procedure and finite element method for the temperature field simulations. The self-developed software has been used. The simulation results, along with their analysis, have been presented.

Keywords: heat transfer, inverse method, solid – solid interface

1. Introduction

In technological process of steel industry heat transfer is a very important factor [1-3]. It plays an essential role especially in metal forming processes. The heat transfer at the solid to solid contact interface is a very common phenomenon. Such situation takes place in metal forming process. The heat transfer between two solid surfaces is a difficult and complex process. There are many physical phenomena which influence the heat flux. Heat transfer occurs by radiation in very thin gap and conduction between the two surfaces brought into contact. Modelling of the temperature field, heat flux or heat transfer coefficient and other phenomena as regards to the process of heat transfer between two solid surfaces has been analysed by several authors, with both commercial software and original formulations having been applied.[4-10].

Determination of heat transfer boundary conditions is necessary to obtain solution to the heat conduction equation in order to obtain the temperature field. The accuracy of result of numerical calculations depends on the proper description of the boundary conditions. Heat flux between a tool and work piece is a function of temperature, pressure and time. For example in the forging process the time of contact between work piece and tool is long and takes about 30 s for a single stroke. Thus, the heat transfer is intensive in such a case. The problem is also highly dependent on surface temperature and contact pressure.

A methodology for the determination of the heat transfer at the contact surface of a pair of samples is presented in the paper. It involves physical experiment and numerical methods. The time dependent temperature profiles have been measured at the experimental stand and inverse method is used to determine the heat flux at the surface of contact.

2. The temperature measurements results

The schematic diagram of the experimental stand is shown in Fig. 1. Furnace has a protective atmosphere made of argon and additionally installed a graphite tube to protect the sample surface against oxidation. In the experiments two samples were used: the Hot sample which has been heated in of the furnace. The second which is named Cold was outside the furnace and has been kept at room temperature. When the Hot sample has reached the desired temperature, the furnace has been opened and the Cold sample was brought into contact with the Hot one at the constant pressure.

In each sample 4 thermocouples were installed with a diameter of 0,5 mm. Geometry of sample and locations of the thermocouples is shown in Fig. 2. Unfortunately, one of the thermocouples was damaged in the Hot sample. During the approach of samples and throughout the test the output of seven thermocouples was monitored and recorded using a computer-based data acquisition system with a frequency of 10 Hz.

* AGH UNIVERSITY OF SCIENCE AND TECHNOLOGY, FACULTY OF METALS ENGINEERING AND INDUSTRIAL COMPUTER SCIENCE, AL. A. MICKIEWICZA 30, 30-059 KRAKÓW, POLSKA

Corresponding author: rywotyc@.agh.edu.pl

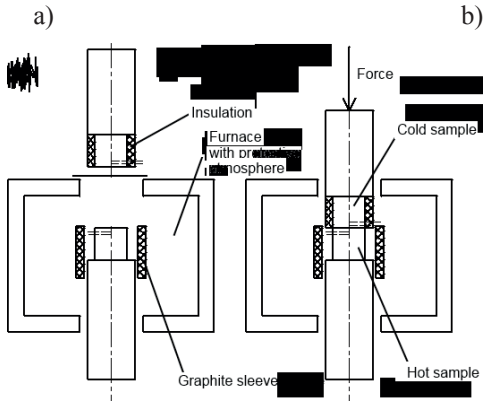

Fig. 1 Schematic diagram of the experiment a) The sample heating in the furnace b) The samples positions during the compression test

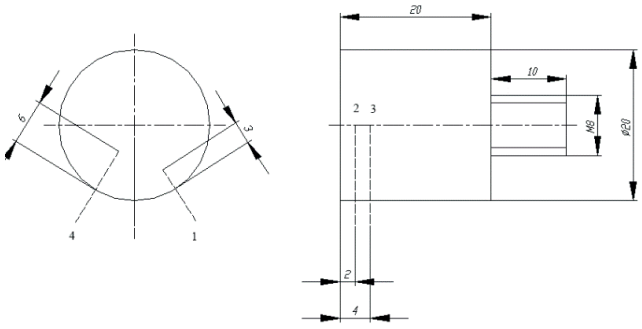

Fig. 2. Geometry of samples and location of thermocouples

The dimensions of samples were as the following: 20 mm in height and 20 mm in diameter. Material of the Cold

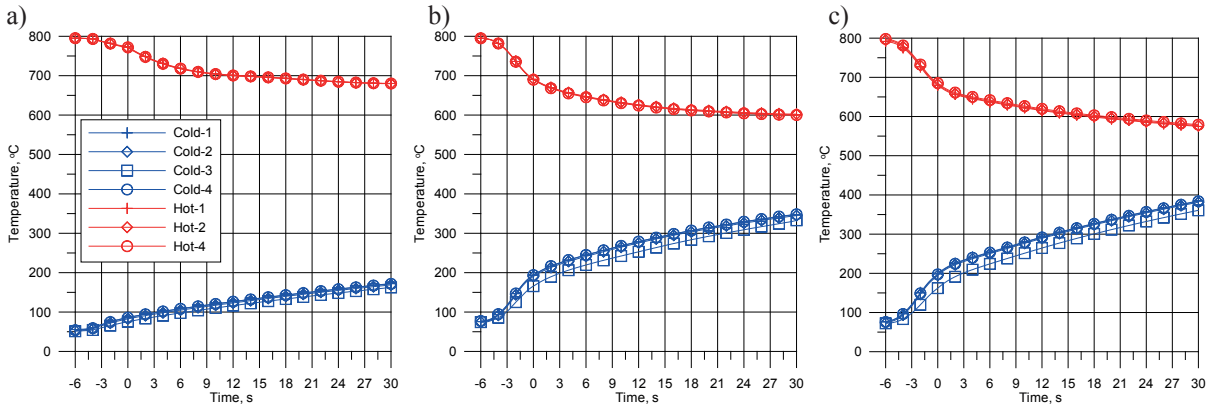

Fig. 3 Temperature distributions in time for the initial sample temperature of 800°C and pressure of :a) – 1 MPa, b) – 10 MPa, c) – 20 MPa

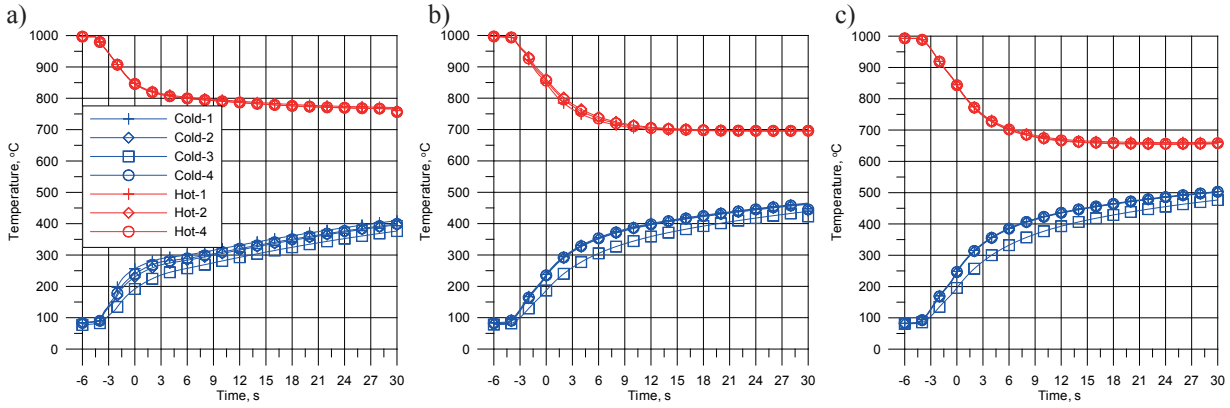

Fig. 4 Temperature distributions in time for the initial sample temperature of 1000°C and pressure of: a) – 1 MPa, b) – 10 MPa, c) – 20 MPa

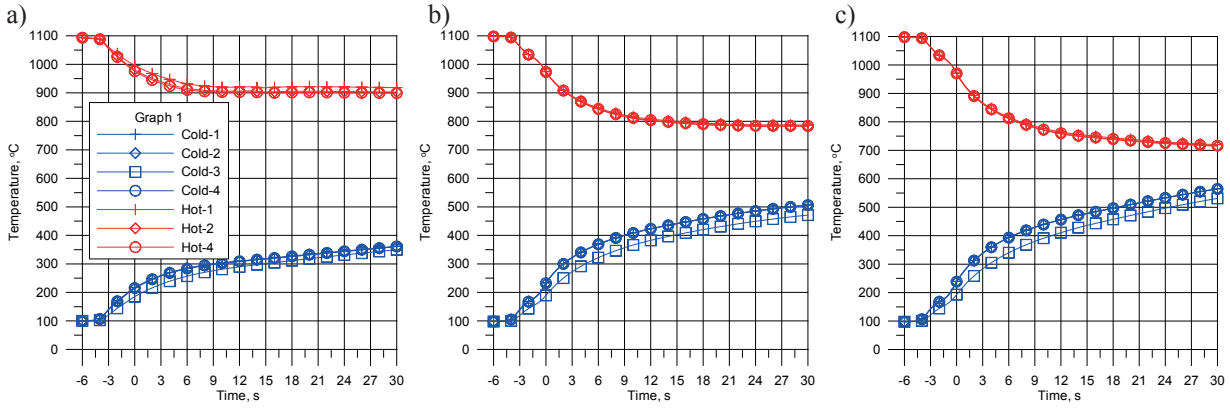

Fig. 5 Temperature distributions in time for the initial sample temperature of 1100°C and pressure of: a) – 1 MPa, b) – 10 MPa, c) – 20 MPa

sample was NC6 steel. The Hot sample was made of C45 steel. The Hot sample has been heated to an initial temperature of: 800°C, 1000°C and 1100°C. The samples have been brought into contact under a pressure of: 1 MPa, 10 MPa and 20 MPa. The samples surfaces were polished after each test and the surface of the Cold samples was cleaned. Time of contact has been equal to 30 s in each test.

The results of temperature measurements for an initial sample temperature of 800°C has been shown in Fig. 3. In Fig. 4, results for the sample temperature of 1000°C and in Fig. 5 for 1100°C have been presented. Increasing the pressure leads to higher temperature of the Cold sample and lower of the Hot sample for each tests.

3. Numerical model

The numerical model consists of the inverse method employed for calculating the heat flux at the interface between Cold and Hot sample. The heat flux at the interface has been determined from the solution to the boundary inverse heat conduction problem. The boundary condition of the heat flux is seeking from temperature variations at points located inside the Cold and Hot samples. The computation algorithm of solving the inverse problem for cooling a three dimensional plate has been given by Malinowski at al. [11]. The necessary modification resulting from reduction of a three dimensional heat conduction problem to the axially symmetrical one will be given. The solution starts with an assumption of a general form of an approximating function of the heat transfer coefficient variation in time. The final aim is to determine the specific form of that function. The objective function has been assumed in the dimensionless form:

$$E(p_i) = \sum_{i=1}^{n}\sum_{j=1}^{m}\left[\frac{t_{ij}^{mea}(\tau) - t_{ij}^{inv}(\tau)}{t_{ij}^{mea}(\tau)}\right]^2 \qquad (1)$$

where:
p_i – vector of the unknown parameters,
$t_{i,j}^{mea}$ – the sample temperature measured by the sensor i at time τ_j,
$t_{i,j}^{inv}$ – the sample temperature at the location of the sensor i at time τ_j calculated from the finite element solution to the sample cooling.

The objective function given by Eq. (1) defines the deference between measured and calculated temperatures. The unknown parameters p_i can be determined by minimizing the objective function. The variable matrix method [12] which utilizes the BFGS updating techniques has been employed. The derivatives of the objective function with respect to the unknown parameters pi have been estimated numerically. The finite difference form of the first derivative is given by:

$$\frac{dE(p_i)}{dp_j} \approx \frac{E(p_i + \Delta p_j) - E(p_i)}{\Delta p_j} \qquad (2)$$

In the approximate expression of the first derivative the increment $\Delta p_j = |p_j|\ 10^{-6}$ has been used.

The temperature field of the Cold and Hot sample is described by the Fourier equation:

$$\frac{\partial T}{\partial \tau} = \frac{\lambda}{c_p \varrho}\nabla^2 T \qquad (3)$$

where:
c_p – specific heat, [J/(kg K)]
λ – heat transfer coefficient, [W/(m K)]
ρ –density, [kg/m^3]
τ – time, [s]
T– temperature, [K]

The temperature field of the sample was determined using an axially symmetrical solution to the heat conduction problem in a cylinder. The finite element discretization of the sample is shown in Fig.6. The description of the finite element model has been given in [13].

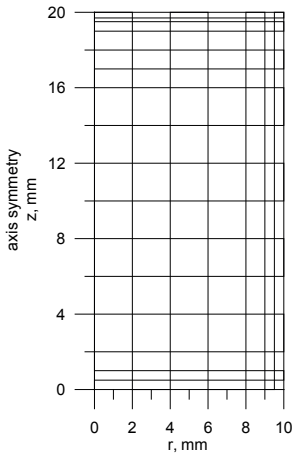

Fig. 6 Finite element mesh employed for the sample discretization

The boundary condition at the contact surface between the Cold and Hot sample has been introduced in the form of heat flux:

$$\dot{q} = h(\tau)(T_s - T_a) \qquad (4)$$

where:
$h(\tau)$ - heat transfer coefficient at the interface. W/m^{2}K
T_s – sample surface temperature, K
T_a – ambient temperature, K

The heat transfer coefficient $h(\tau)$ has been approximated by the cubic spline functions:

$$h(\tau) = \sum_{j=1}^{4} H_j(\eta)p_j \qquad \text{for } \eta \in (0,1). \qquad (5)$$

Accuracy of the heat transfer coefficient approximation in time has been controlled dividing the time of contact into periods for which $\tau \in (\tau_1,\tau_2)$. The local coordinate h is given by:

$$\eta = \frac{\tau - \tau_1}{\tau_2 - \tau_1} \tag{6}$$

The cubic spline functions H_j have the following form:

$$H_1 = 1 - 3\eta^2 + 2\eta^3$$

$$H_2 = 3\eta^2 - 2\eta^3 \tag{7}$$

$$H_3 = \eta - 2\eta^2 + \eta^3$$

$$H_4 = -\eta^2 + \eta^3$$

The parameters p_j define at nodes of approximation the values of the heat transfer coefficient at the samples interface and its derivatives with respect to time.

Boundary conditions at the sample side surfaces have been introduced in the following form:

$$\dot{q_{ss}} = h_{ss}(T_{ss} - T_a) \tag{8}$$

where:
h_{ss} - heat transfer coefficient at the side surface, W/m^{2}K
T_{ss} – side surface temperature of the Hot or Cold sample, K

At the bottom surface of each sample the heat flux has been defined:

$$\dot{q_b} = h_b(T_b - T_a) \tag{9}$$

where:
h_b - heat transfer coefficient at the bottom surface, W/m^{2}K
T_b – bottom surface temperature of the Hot or Cold sample, K

The boundary conditions at the side surfaces have a strong influence on the accuracy of the inverse solution. To complete the boundary conditions, the heat transfer coefficients h_{ss}, h_b has been specified. For the Hot sample the following relations

$$h_{ss} = \left(1.2 - 0.52\frac{T_{ss}}{1000}\right) \cdot 5.675 * 10^{-8}\frac{T_{ss}^4 - T_a^4}{T_{ss} - T_a} \tag{10}$$

$$h_b = 300 \text{ W/m}^2\text{K} \tag{11}$$

have been used in the calculations [4]:

The semi-empirical equation:

$$h_{ss} = h_{rad} + h_{con} \tag{12}$$

where:

$$h_{rad} = 0.6 \cdot 5.675 \cdot 10^{-8}\frac{T_{ss}^4 - T_a^4}{T_{ss} - T_a} \tag{13}$$

and

$$h_{con} = \left(-2.93 * 10^{-11} * t_{ss}^4 + 2.51 * 10^{-8} * t_{ss}^3 - 7.27 * 10^{-6} * t_{ss}^2 + 8{,}87 * 10^{-4} * t_{ss} - 2.83 * 10^{-2}\right)^{-1} \tag{14}$$

and
$t_{ss} = T_{ss}$-273

have been used at the side surface of the Cold sample. The boundary conditions at the side surface of the cold sample take into account heat losses due to radiation and conduction to the insulation. At the bottom surface of the Cold sample the empirical equation has been employed [5]:

$$h_b = 300 \cdot \left(1 + \frac{\tau}{50}\right) \tag{15}$$

where:
τ - time, s

The samples material properties, necessary to solve the problem have been expressed as functions of temperature [14].

4. Numerical computations and results

The results of numerical calculations have been presented in Fig. 7. The calculation results have allowed the determination of heat flux for all the cases. The Fig. 7 shows heat flux variations in time. As the contact pressure increases, the heat flux also increases. Higher initial temperature of the sample has given higher heat flux. The heat transfer was more intensive if the temperature difference was higher. The heat flux strongly depends on the contact pressure and initial temperature of the Hot sample. There are only minor differences of the heat fluxes curves determined from the inverse solution to the Cold and Hot sample. Same differences are due to the difficulties in the description of the boundary conditions for the Cold sample which has been inserted into the extremely hot furnace.

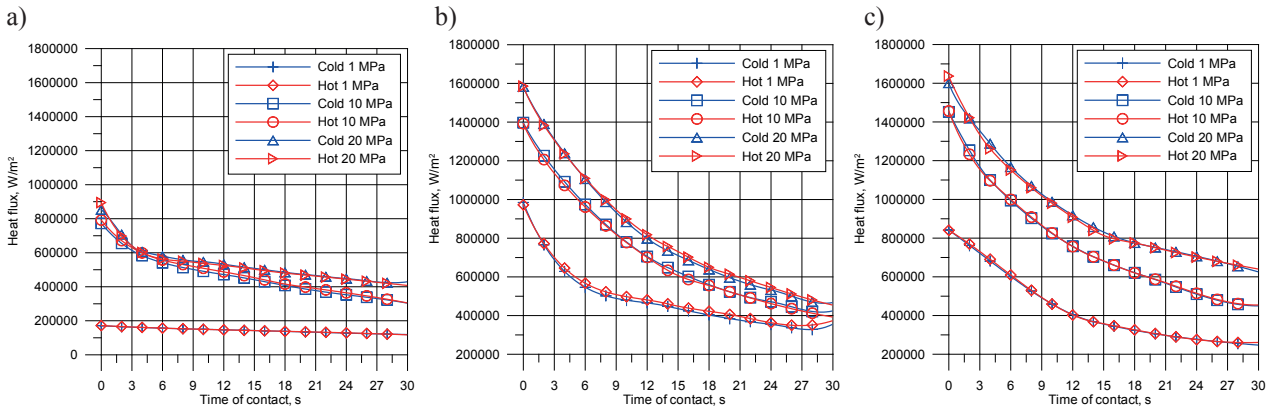

Fig. 7 Heat flux as function of time for the initial sample temperatures of: a) 800°C, b) 1000°C c) 1100°C

The average deviation of the computed temperatures from the measured ones has been presented in Table 1. For all the cases the temperature difference is lower than 4°C. The accuracy of the determination of the temperature fields from the inverse solution is at acceptably level. The final temperature fields shown in Fig. 8 to Fig. 10 for both samples are correct. The shape of isotherm is typical for the examined heat transfer problem.

TABLE 1

The average deviation of the calculated temperatures from the measured temperature histories.

Initial temperature of the Hot sample	Sample	Contact pressure		
		1 MPa	10 MPa	20 MPa
800°C	Cold	1.571°C	1.589°C	1.677°C
	Hot	0.767°C	1.232°C	2.363°C
1000°C	Cold	2.449°C	3.667°C	0.709°C
	Hot	0.770°C	1.736°C	0.468°C
1100°C	Cold	3.976°C	2.375°C	0.484°C
	Hot	0.405°C	0.647°C	0.636°C

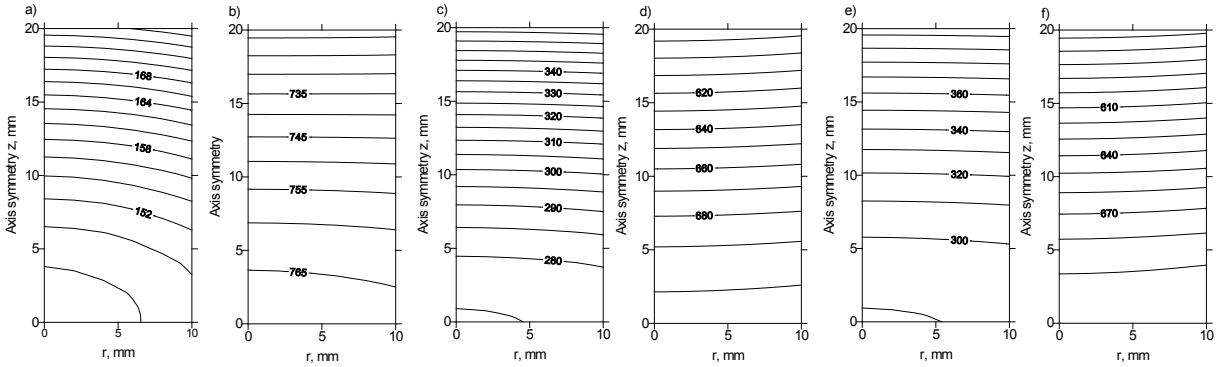

Fig. 8 Temperature fields for test of an initial Hot sample temperature of 800°C a) Cold – 1 MPa, b) Hot – 1 MPa, c) Cold – 10 MPa, d) Hot – 10 MPa, e) Hot – 20 MPa, f) Cold – 20 MPa

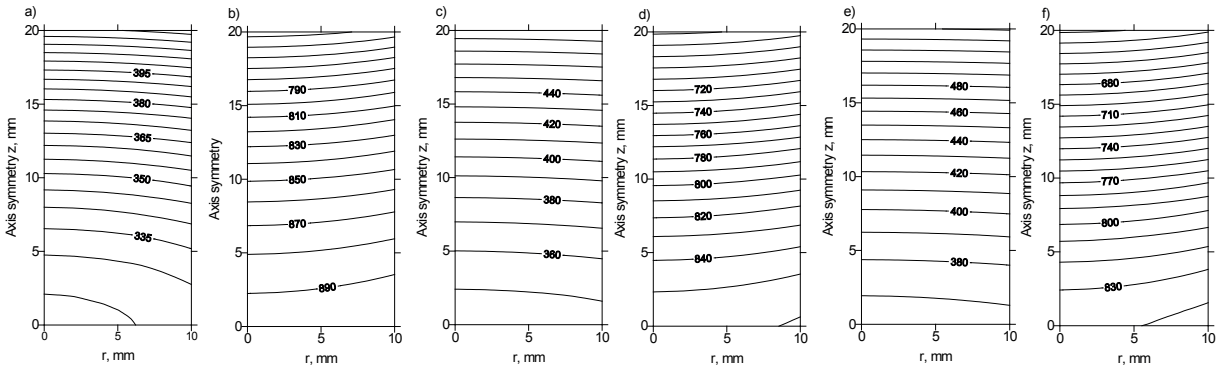

Fig. 9 Temperature fields for test of an initial Hot sample temperature of 1000°C a) Cold – 1 MPa, b) Hot – 1 MPa, c) Cold – 10 MPa, d) Hot – 10 MPa, e) Hot – 20 MPa, f) Cold – 20 MPa

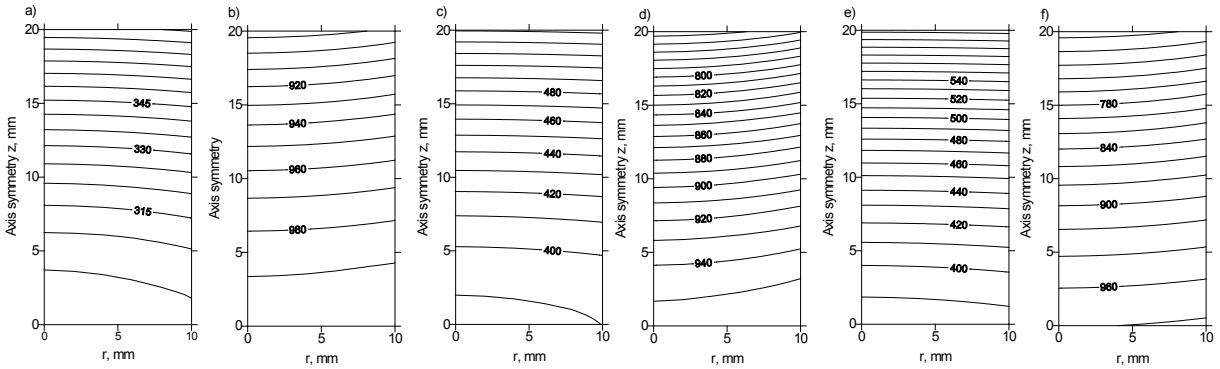

Fig. 10 Temperature fields for test of an initial Hot sample temperature of 1100°C a) Cold – 1 MPa, b) Hot – 1 MPa, c) Cold – 10 MPa, d) Hot – 10 MPa, e) Hot – 20 MPa, f) Cold – 20 MPa

5. Conclusion

The methodology for the determination of the heat transfer coefficient at solid to solid interface has been developed. It involves physical experiment and numerical methods. The first one requires measurements of the temperature variations at specified points at two samples brought into contact. The numerical part makes use of the inverse method for calculating the heat flux and heat transfer coefficient at samples interface.

Correct results have been obtained for all samples and cases as regards to the heat flux. The next stage of research will be focused in determining the heat transfer coefficient as empirical relationships of the sample surface temperatures and pressures for the Hot and Cold samples, which model the tool and work piece.

Acknowledgments

The study performed as part of the regular activity, AGH University of Science and Technology, Faculty of Metals Engineering and Industrial Computer Science, Work No. 11.11.110.226.

REFERENCES

[1] K. Miłkowska-Piszczek, J. Falkus, Metalurgija **53**, 4, 571-573 (2014).

[2] Hadala, B Cebo-Rudnicka, Malinowski, Goldasz, Archives of Metallurgy and Materials **56** (2) 367-377 (2011).

[3] M. Hojny, M. Glowacki, Archives of Metallurgy and Materials **54**, 2, 475–483 (2009).

[4] Z. Malinowski, J.G. Lenard, M.E. Davies, Journal Of Materials Processing Technology **41**, (2), 125-142, (1994).

[5] L.Galdos, E. Saenz de Argandona, J. Mendiguren, R. Ortubay, X. Agirretxe, J.M. Martin, Computer Methods in Materials Science **15**, (1), 58-64 (2015).

[6] M. Rosochowska, K. Chodnikiewicz, R. Balendra, Journal of Materials Processing Technology **145**, 207–214 (2004).

[7] A. Blaise, B. Bourouga, B. Abdulhay, C. Dessain, Applied Thermal Engineering **61**, 141-148 (2013).

[8] M. Rosochowska, R. Balendra, K. Chodnikiewicz, Journal of Materials Processing Technology **135**, 204–210 (2003).

[9] C.C. Chang, A.N. Bramley, Proceedings of the Institution of Mechanical Engineers **216**, (8), 1179-1186 (2002).

[10] P. Salomonsson, M. Oldenburg, P. Åkerström, G. Bergman, Steel Research Int. **80**, (11), 841-845 (2009).

[11] Z. Malinowski, T. Telejko, B. Hadała, A. Cebo-Rudnicka, A. Szajding, International Journal of Heat and Mass Transfer **75**, 347–361 (2014).

[12] T. Kręglewski, T. Rogowski, A. Ruszczyński, J. Szymanowski, Metody optymalizacji w języku FORTRAN, PWN, Warszawa1984.

[13] Z. Malinowski, Archives of Metallurgy **46**, 93-118 (2001).

[14] Z. Malinowski, Numeryczne modele w przeróbce plastycznej i wymianie ciepła. AG H UWN -D, Kraków, 2005.

Received: 10 March 2015.